



## Genitourinary and Gynecologic Imaging Original Research

# Multiparametric magnetic resonance imaging for characterizing renal tumors: A validation study of the algorithm presented by Cornelis *et al.*

Pia Iben Pietersen<sup>1</sup>, Janni Lynggård Bo Madsen<sup>2</sup>, Jon Asmussen<sup>1</sup>, Lars Lund<sup>3</sup>, Tommy Kjærgaard Nielsen<sup>4</sup>, Michael Pedersen<sup>5</sup>, Birte Engvad<sup>6</sup>, Ole Graumann<sup>1</sup>

<sup>1</sup>Department of Radiology, Odense University Hospital, <sup>2</sup>Research and Innovation Unit, Department of Clinical Research, University of Southern Denmark, <sup>3</sup>Department of Urology, Odense University Hospital, Odense, <sup>4</sup>Department of Urology, Aarhus University Hospital, <sup>5</sup>Department of Clinical Medicine - Comparative Medicine Lab, Aarhus University Hospital, Aarhus, <sup>6</sup>Department of Pathology, Odense University Hospital, Odense, Denmark.



### \*Corresponding author:

Pia Iben Pietersen,  
Department of Radiology,  
Odense University Hospital,  
Odense, Denmark.

[pia.iben.pietersen3@rsyd.dk](mailto:pia.iben.pietersen3@rsyd.dk)

Received : 15 October 2022  
Accepted : 17 January 2023  
Published : 02 February 2023

DOI  
10.25259/JCIS\_124\_2022

### Quick Response Code:



## ABSTRACT

**Objectives:** In the last decade, the incidence of renal cell carcinoma (RCC) has been rising, with the greatest increase observed for solid tumors. Magnetic resonance imaging (MRI) protocols and algorithms have recently been available for classifying RCC subtypes and benign subtypes. The objective of this study was to prospectively validate the MRI algorithm presented by Cornelis *et al.* for RCC classification.

**Material and Methods:** Over a 7-month period, 38 patients with 44 renal tumors were prospectively included in the study and received an MRI examination in addition to the conventional investigation program. The MRI sequences were: T2-weighted, dual chemical shift MRI, diffusion-weighted imaging (DWI), and dynamic contrast-enhanced T1-weighted in wash-in and wash-out phases. The images were evaluated according to the algorithm by two experienced, blinded radiologists, and the histopathological diagnosis served as the gold standard.

**Results:** Of 44 tumors in 38 patients, only 8 tumors (18.2%) received the same MRI diagnosis according to the algorithm as the histopathological diagnosis. MRI diagnosed 16 angiomyolipoma, 14 clear cell RCC (ccRCC), 12 chromophobe RCC (chRCC), and two papillary RCC (pRCC), while histopathological examination diagnosed 24 ccRCC, four pRCC, one chRCC, and one mixed tumor of both pRCC and chRCC. Malignant tumors were statistically significantly larger than the benign ( $3.16 \pm 1.34$  cm vs.  $2.00 \pm 1.04$  cm,  $P = 0.006$ ).

**Conclusion:** This prospective study could not reproduce Cornelis *et al.*'s results and does not support differentiating renal masses using multiparametric MRI without percutaneous biopsy in the future. The MRI algorithm showed few promising results to categorize renal tumors, indicating histopathology for clinical decisions and follow-up regimes of renal masses are still required.

**Keywords:** Kidney, Magnetic resonance imaging, Imaging sequences, Urinary, Neoplasms-primary

## INTRODUCTION

As a result of the increased and widespread use of cross-sectional imaging as computed tomography (CT) and magnetic resonance imaging (MRI), the number of incidental renal masses has increased.<sup>[1,2]</sup> These incidental renal masses vary from benign cysts to renal cell carcinomas (RCCs), having variable aggressiveness and metastatic progression potential.<sup>[3]</sup> RCC occurs in different forms, of which clear cell RCC (ccRCC) is the most common, followed by

This is an open-access article distributed under the terms of the Creative Commons Attribution-Non Commercial-Share Alike 4.0 License, which allows others to remix, transform, and build upon the work non-commercially, as long as the author is credited and the new creations are licensed under the identical terms.

©2023 Published by Scientific Scholar on behalf of Journal of Clinical Imaging Science

papillary and chromophobe RCCs (chRCC).<sup>[4]</sup> The subtypes of RCC exhibit different biologic behavior in terms of growth rate and treatment response, as well as different prognoses.<sup>[5,6]</sup> It is therefore crucial to determine the specific subtype to determine the optimal therapeutic approach.

Current diagnostic guidelines for differentiating subtypes include a histopathological examination. Recent studies have suggested the use of multiparametric MRI combined with the administration of a contrast agent as a diagnostic method capable of differentiating between benign and malignant renal tumours.<sup>[7-11]</sup> If proved accurate, multiparametric MRI of renal tumors could provide new *in vivo* information regarding tumor type, decreasing the need for percutaneous histopathological biopsy and thereby decreasing the risk for resulting complications.<sup>[12-17]</sup>

In 2017, Cornelis and Grenier presented a practical algorithm for classifying renal tumors, differentiating between RCC and benign subtypes using multiparametric MRI.<sup>[18]</sup> The algorithm consists of five individual MRI sequences designed to classify ccRCC, papillary RCC (pRCC), chRCC, oncocytoma (OC), and angiomyolipoma (AML). These sequences are T2 weighted, dual chemical shift MRI, diffusion-weighted imaging (DWI), and dynamic contrast-enhanced (DCE) T1 in both the wash-in and wash-out phases. According to Cornelis *et al.*, the sequences must be read in this specific order to differentiate one subtype from another, as well as for a standardized approach. The algorithm is based solely on a theoretical review of published papers and has not previously been investigated in a clinical and research setting. The aim of this study was therefore two-fold: To collect validity evidence by testing MRI sequences according to Cornelis *et al.*'s algorithm regarding the classification of renal tumor subtypes, and to compare those results with the post-operative histopathological results. The hypothesis was that the MRI protocol could correctly classify a majority of the subtypes.

## MATERIAL AND METHODS

### Setting

The study was conducted and the manuscript prepared according to the Strengthening the Reporting of Observational studies in Epidemiology guidelines.<sup>[19]</sup> The prospective and cohort study was carried out at Odense University Hospital, Denmark over a period of 7 months between May 2017 and December 2017. Patients in the fast-track program for suspected renal cancer were recruited, and before any biopsy and histopathological evaluation, each was administered an MRI scan with the sequences included in the algorithm.

This study was approved by The National Committee on Health Research Ethics, The Danish Data Protection Agency

(no: 17/5113), and the Danish Patient Safety Authority. All participants provided informed oral and written consent before inclusion.

### Patients

Consecutive patients in a fast-track program for the investigation of renal tumors were prospectively recruited from the hospital's urology outpatient clinic. Patients were eligible if all of the following criteria were met:

- Presentation of suspected renal tumor either found by computed CT or ultrasound, and
- Age  $\geq 18$  years, and
- Normal kidney function defined as estimated glomerulus filtration ratio  $\geq 60$  mL/min/1.73 m<sup>2</sup>, and
- Informed consent understood and provided.

Exclusion criteria were: Pregnancy, graft kidney, contrast allergy, patients with non-MRI-compatible components, or the inability to meet a patient's fast-track guarantee for diagnosing renal tumors within a stated time frame.

Included patients were offered an additional MRI examination with the experimental sequences on the same day of the biopsy but before the invasive procedure. [Figure 1] presents the flowchart of patients included in the study. Histopathological diagnosis, obtained either from a subsequent percutaneous biopsy or surgical radical or partial nephrectomy, served as the gold standard.

### MRI

All MRI examinations were performed using a clinical 3.0 T system (Ingenia, Phillips Healthcare, Best, Netherlands) with a 32-channel large anterior surface body coil combined with a posterior moveable coil. The respiration triggering device was placed under the anterior coil at the diaphragm level. All

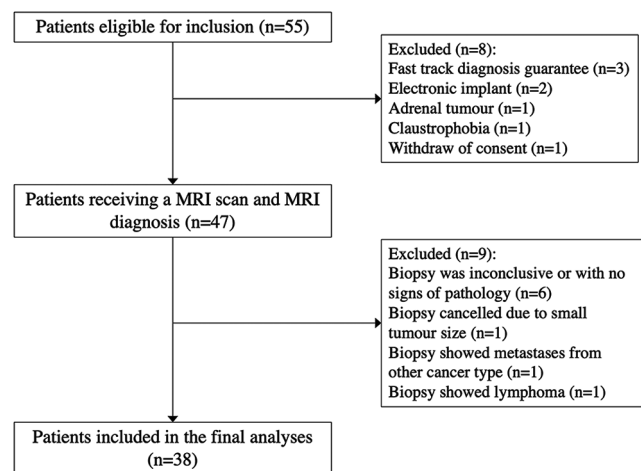


Figure 1: Patient flowchart.

patients underwent a survey in two plans with the respiration trigger and two plans with breath-hold, respiration triggered T2-weighted (T2w) turbo spin-echo sequence in transversal and coronal plan, a fat-suppressed diffusion-weighted imaging (DWI) sequence in the transverse plane, and T1-weighted (T1w) DIXON sequence performed both before and 25 s after administration of a gadolinium-containing agent for corticomedullary phase as well as at 120 s after administration for the nephrographic phase. The MRI protocol is presented in [Table 1]. The contrast agent was injected rapidly through an antecubital vein and

immediately followed by a flush of 30 mL saline solution (0.9% NaCl). Gadovist (Bayer, Leverkusen, Germany) was used as a contrast agent and administered at 0.1 mL/kg, and a maximum of 7.5 mL was injected. For all MRI sequences, sensitivity encoding was used. [Figure 2] presents the sequences used in the assessments according to Cornelis' proposed algorithm.

Before receiving histopathology results and diagnosis, two radiologists (OG and JTA), with 9 and 14 years MRI experience in the interpretation of renal tumors, assessed

**Table 1:** MRI sequence parameters for RCC protocol.

MRI sequences					
MRI protocol	BTFE	DWI	T1-Weighted DIXON	T2 MVXD	T2-Weighted
Plane	Coronal	Transverse	Transverse	Transverse	Coronal
Fat saturation	No	Yes	No	No	No
TR (ms)	3.5	1940	3.7	2725	4960
TE (ms)	1.75	83	1.31	135	80
Angulation (°)	45	90	10	90	90
Thickness (mm)	8	4	3	4	3
Matrix (mm×mm <sup>2</sup> )	351×229	400×200	405×199.5	400×199	499×118.5
Scanning time (s)	28	297	18	306	49
Delay (s)			0, 25, 120		
b-values (s/mm <sup>2</sup> )		0, 150, 1000			

RCC: Renal cell carcinoma, MRI: Magnetic resonance imaging

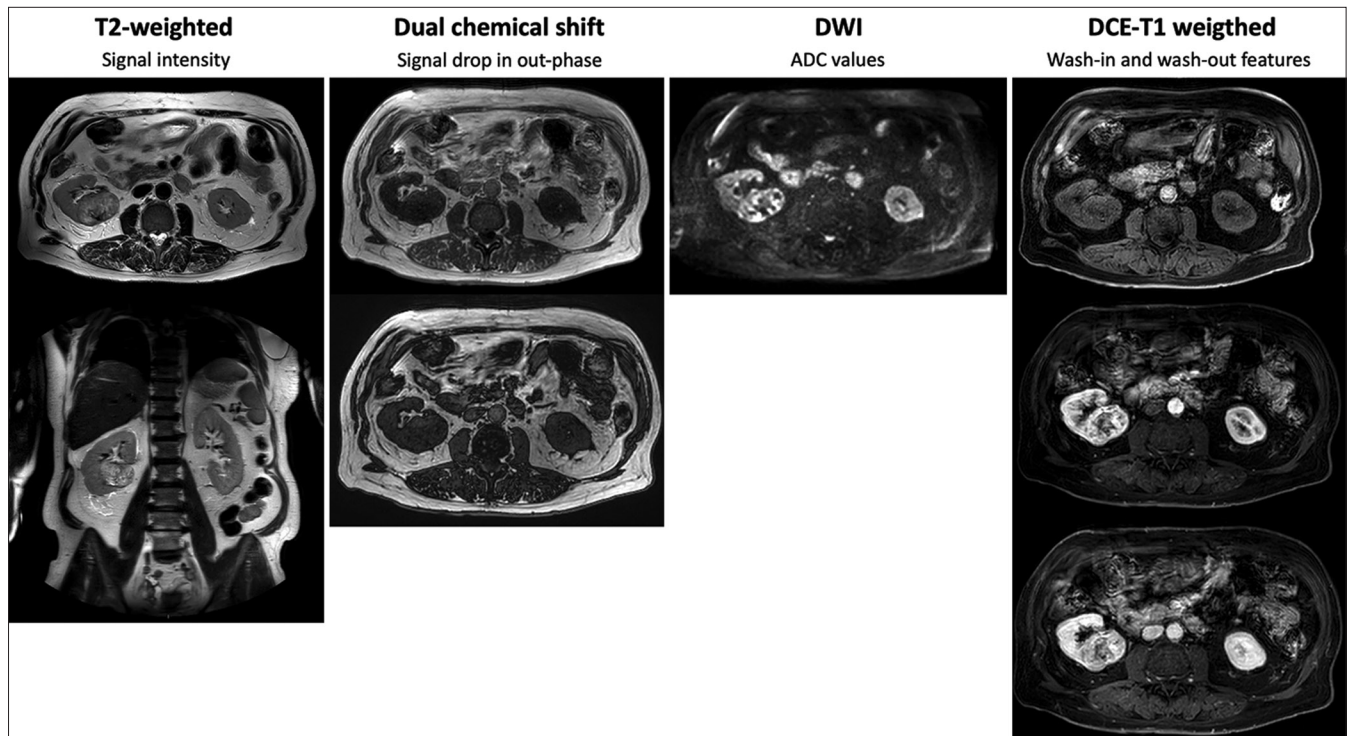


**Figure 2:** Magnetic resonance imaging sequences assessed in the algorithm including T2-weighted, Dual chemical shift, Diffusion-weighted imaging (DWI), Dynamic contrast-enhanced (DCE) T1-weighted in in-and out-phase.

**Table 2:** The practical MRI algorithm proposed by Cornelis *et al.*

Order	Sequences	Imaging features	Results		
1	T2w	Signal intensity <sup>Ⓞ</sup>	High cc-RCC/OC	Mid Ch-RCC	Low AML/p-RCC
2	Dual chemical shift MRI	Signal drop on out-phase	Yes cc-RCC/AML	-	No OC/p-RCC
3	DWI	ADC <sup>†</sup>	High OC/cc-RCC	Mid Ch-RCC	Low AML/p-RCC
4	DCE-T1w	Wash-in	Fast and intense cc-RCC/AML	Mid and delayed Ch-RCC/OC	Slow p-RCC
5	DCE-T1w	Wash-out	Yes cc-RCC/AML	Mid Ch-RCC/OC	No P-RCC

<sup>Ⓞ</sup>Compared to renal cortex, <sup>†</sup>Apparent diffusion coefficient, T2W: T2 weighted images, ccRCC: Clear cell renal cell carcinoma, OC: Oncocytoma, ChRCC: Chromophobe renal cell carcinoma, AML: Angiomyolipoma, pRCC: Papillary renal cell carcinoma, DWI: Diffusion-weighted imaging, ADC: Apparent diffusion coefficient, DCE: Dynamic contrast enhanced, T1w: T1-weighted, MRI: Magnetic resonance imaging

and described in consensus the images in the prescribed order. For each tumor, the radiologists evaluated tumor appearance, one sequence at a time, according to Cornelis *et al.*'s algorithm [Table 2].<sup>[18]</sup> If an MRI diagnosis was established after 1–4 sequences, all remaining sequences were still evaluated. For example, high signal intensity in the first sequence (T2w) suggests cc-RCC or OC, [Table 2]. If the tumor shows a signal drop on the out-phase on the second sequence (dual chemical shift MRI), cc-RCC or AML is suggested. The combination of the first two sequences excludes all remaining tumor types, and cc-RCC is proposed as the diagnosis. In another scenario, a tumor might present intermediate/middle intensity during the first sequence, suggesting Ch-RCC. In these instances, images from all remaining sequences were still evaluated.

Tumor size was measured in two dimensions on the transverse T2w image: medial-lateral and anterior-posterior, where the largest diameter was noted.

### Histopathological analyses

The histopathological diagnosis was considered the gold standard. Histopathology diagnosis was available for all tumors after percutaneous biopsy samples were obtained using an 18-gauge semiautomatic side-cutting needle (SemiCut, MDL, Delebio, Italy). At least two samples of each tumor were obtained and analyzed according to the World Health Organization guidelines by a pathologist with more than 4 years of specialized experience in diagnosing renal tumors.

### Statistical analysis

All patient data were retrieved by one author (JLBM) through a review of medical records and pathology reports

(tumor subtype and treatment). All data were collected and managed using Research electronic data capture,<sup>[20]</sup> an electronic data capture tool hosted at Odense Patient Data Explorative Network. Descriptive statistics, including percentages, means, range, and standard deviations, were calculated for the demographic variables, and the percentage of correctly or incorrectly classified tumors was reported.

All data analyses were performed using STATA 16 (StataCorp; Stata Statistical Software: Release 15. College Station, TX: StataCorp LLC).

## RESULTS

### Patients

A total of 55 patients were eligible for inclusion in the study period and of these, 38 patients were included in the final analyses, [Figure 1]. The mean age of the patients was 66.8 years (range 43–79, SD ± 8.31), and 21.1% were women (*n* = 8). The 38 patients had a total of 44 tumors, with one patient who had three tumors and four patients with two tumors each. All included tumors were histopathologically diagnosed – either from a biopsy alone (*n* = 29, 65.9%) or including post-surgery excision (*n* = 15, 34.1%). The patient demographic is presented in [Table 3].

### MRI diagnoses according to the algorithm

The assessment results and MRI diagnoses according to the sequential approach of the algorithm are presented in [Table 4]. The assessments revealed 16 AML, 14 ccRCC, 12 chRCC, and two pRCC. Two tumors could not be successfully classified due to significant heterogeneity (tumor ID: 1 and 13). Tumor 1 was classified independently of the *not reported sequence* because it showed a medium

**Table 3:** Patient demographic ( $n=38$ ).

Age, years (mean $\pm$ SD)	66.8 $\pm$ 8.3
Gender (n, %)	
Female	8 (21.1)
Male	30 (78.9)
Body mass index (mean $\pm$ SD)	27.6 $\pm$ 4.2
Treatment (n, %)	
Cryoablative therapy	15 (39.5)
Partial nephrectomy	5 (13.1)
Radical nephrectomy	3 (7.9)
Active surveillance	15 (39.5)
SD: Standard deviation	

signal intensity in the first sequence, which would indicate a diagnosis of chRCC. Tumor ID 13 was assessed with low signal intensity on T2w images, was not possible to assess in the dual chemical shift MRI, and showed ADC value on DWI. Since the different sequence assessments indicated different diagnoses, a unanimous diagnosis could not be reached.

### Histopathological results

The histopathological examinations, used as the gold standard, revealed 68.2% of the tumors were malignant, consisting of 24 ccRCC, four pRCC, one chRCC, and one mixed tumor of both pRCC and chRCC. The benign tumors accounted for the remaining 31.8% and consisted of two AML and 12 OC. Most of the tumors were inhomogeneous (70.5%), and the majority did not contain cystic elements (75.0%). The mean RENAL nephrometry score was  $7.4 \pm 2.4$ , ranging from 4 to 12. The mean size for all tumors was  $2.80 \pm 1.36$  cm (1–9 cm). The malignant tumors were significantly larger than the benign tumors, with a mean size of  $3.16 \pm 1.34$  cm versus  $2.00 \pm 1.04$  cm, respectively, compared using a non-paired students *t*-test,  $P = 0.006$ . The mean size of the subtypes OC and ccRCC were  $2.00 \pm 1.04$  cm and  $3.13 \pm 1.39$  cm, respectively.

In total, eight tumors of 44 (18.2%) were correctly classified: five ccRCC (tumor ID: 10, 14, 17, 23, and 27), one Ch-RCC (tumor ID: 3), one pRCC (tumor ID: 32), and one AML (tumor ID 36).

### The overall accuracy of the algorithm

After the primary analyses, we performed a retrospective analysis and for each tumor evaluated whether each specific sequence and assessment were correct according to the algorithm. In total, 49.8% of the MRI sequence assessments were correct according to histopathological diagnosis [Table 5].

Using the algorithm, the T2w sequence correctly assessed 20 of 43 tumors, which corresponds to a percentage of agreement

of 46.5%. The dual chemical shift sequence had a percentage of agreement of 62.8%, and the DWI sequence had a percentage of agreement of 48.8%. The last two sequences, the DCE-T1w wash-in and wash-out, also revealed a low percentage of agreement retrospectively in all sequences: 48.8% and 41.9%, respectively. [Table 5] presents the retrospective comparison of histopathological results with the algorithm divided by benign/malignant and tumor subtypes.

### DISCUSSION

In this study, the diversity of both benign and malignant renal tumors' MRI patterns in different sequences was prospectively explored regarding the practical algorithm proposed by Cornelis and Grenier.<sup>[18]</sup> Remarkably, we were unable to reproduce the results from the original paper and were unable to correctly differentiate between the subtypes of renal tumors using the multiparametric MRI sequence algorithm. To the best of our knowledge, this is the first prospective study attempting to validate an MRI protocol for differentiating between renal tumor subtypes. Cornelis *et al.* recommend a structured step-by-step process of five sequences to differentiate between renal tumor subtypes using the resulting images. The sequences include: (1) Signal intensity compared to the renal cortex in the T2w sequence, (2) signal drop in out-phase of the dual chemical shift MRI sequence, (3) ADC calculation from images acquired with the DWI sequence, (4) wash-in analysis of a DCE T1w sequence, and (5) wash-out analysis of a DCE T1w sequence.

*In vivo* characterization of tumors is of paramount importance, and image-guided characterization would decrease the use of percutaneous biopsies and the resulting complications. In our prospective study, the multiparametric MRI sequences correctly classified only eight tumors; therefore, the results do not provide sufficient evidence to recommend relying on MRI as a diagnostic imaging technique as opposed to invasive procedures and histopathological examinations. A major challenge to the algorithm, and subsequently a challenge to the conduction of our study, is the indefinite description of the categoric classification in each tumor subtype's profiles. The algorithm does not propose any specific or quantitative measures, for example, defining ADC values as high, middle, or low; or characterizing a DCE-T1w wash-in phase as *fast and intense* or *mid and delayed*. As a result, the assessments can be affected by a subjective judgment or institutional cultural differences, among other factors.

Several studies have recently suggested different approaches for using multiparametric MRI to differentiate between renal masses, either as a dichotomic outcome (benign versus malignant) or by distinguishing between benign or malignant subtypes.<sup>[21-24]</sup> The content of these approaches varies from 3 to 11 MRI sequences and assessments, and includes both categoric and dichotomic assessments. Kay *et al.* also begin

**Table 4:** MRI assessments and diagnoses according to the algorithm.

ID	T2	MR diagnosis	Dual Signal drop	MR diagnosis	DWI	DCE-T1w wash in	DCE-T1w wash out	MRI diagnosis	Histopathologic diagnosis	Correct diagnosis
1	Middle	Ch-RCC	N/R	-	Middle	Fast and intense	Middle	Ch-RCC	cc-RCC	
2	Low	-	Yes	AML	High	Slow	Yes	AML	cc-RCC	
3	Middle	Ch-RCC	Yes	-	High	Slow	Yes	Ch-RCC	Ch-RCC	☺
4	Middle	Ch-RCC	Yes		High	Mid and delayed	Yes	Ch-RCC	cc-RCC	
5	Low	-	Yes	AML	High	Slow	Yes	AML	cc-RCC	
6	Low	-	Yes	AML	High	Fast and intense	No	AML	OC	
7	Low	-	Yes	AML	Middle	Mid and delayed	Yes	AML	cc-RCC	
8	Low	-	Yes	AML	Low	Slow	Yes	AML	p-RCC	
9	Middle	Ch-RCC	Yes		High	Fast and intense	Middle	Ch-RCC	cc-RCC	
10	High	-	Yes	cc-RCC	High	Fast and intense	No	cc-RCC	cc-RCC	☺
11	Middle	Ch-RCC	Yes		Middle	Mid and delayed	Middle	Ch-RCC	cc-RCC	
12	High		Yes	cc-RCC	Middle	Mid and delayed	Middle	cc-RCC	OC	
13	Low	-	N/R	-	High	-	-	AML ?	Mixed tumour	
14	High		Yes	cc-RCC	Middle	Fast and intense	No	cc-RCC	cc-RCC	☺
15	Low		Yes	AML	Middle	Fast and intense	No	AML	cc-RCC	
16	Middle	Ch-RCC	Yes		High	Mid and delayed	Yes	Ch-RCC	cc-RCC	
17	High		Yes	cc-RCC	Middle	Slow	Yes	cc-RCC	cc-RCC	☺
18	Middle	Ch-RCC	N/R		Middle	Fast and intense	No	Ch-RCC	AML	
19	High		Yes	cc-RCC	Middle	Fast and intense	Middle	cc-RCC	OC	
20	Middle	Ch-RCC	Yes		High	Slow	Yes	Ch-RCC	cc-RCC	
21	Middle	Ch-RCC	Yes		High	Fast and intense	Middle	Ch-RCC	cc-RCC	
22	Middle	Ch-RCC	Yes		Low	Fast and intense	Middle	Ch-RCC	cc-RCC	
23	High		Yes	cc-RCC	High	Fast and intense	Middle	cc-RCC	cc-RCC	☺
24	Low		Yes	AML	Middle	Fast and intense	No	AML	cc-RCC	
25	Low		Yes	AML	High	Fast and intense	No	AML	OC	
26	High		Yes	cc-RCC	Middle	Fast and intense	Middle	cc-RCC	OC	
27	High		Yes	cc-RCC	Middle	Slow	Middle	cc-RCC	cc-RCC	☺
28	High		Yes	cc-RCC	High	Slow	Middle	cc-RCC	OC	
29	Low		Yes	AML	Middle	Slow	Yes	AML	p-RCC	
30	Low		Yes	AML	High	Mid and delayed	Middle	AML	cc-RCC	
31	Low		Yes	AML	High	Fast and intense	Middle	AML	cc-RCC	
32	Low		No	P-RCC	Low	Mid and delayed	Yes	p-RCC	p-RCC	☺
33	Low		Yes	AML	Middle	Mid and delayed	Middle	AML	OC	
34	High		Yes	cc-RCC	Middle	Fast and intense	Middle	cc-RCC	OC	
35	Low		Yes	AML	Middle	Mid and delayed	Middle	AML	cc-RCC	
36	Low		Yes	AML	Low	Mid and delayed	Yes	AML	AML	☺
37	High		Yes	cc-RCC	High	Mid and delayed	Middle	cc-RCC	OC	
38	Low		No	P-RCC	Low	Fast and intense	Middle	P-RCC	cc-RCC	
39	Middle	Ch-RCC	Yes		Middle	Fast and intense	Middle	Ch-RCC	cc-RCC	
40	High		Yes	cc-RCC	Middle	Fast and intense	No	cc-RCC	OC	
41	High		Yes	cc-RCC	High	Mid and delayed	Middle	cc-RCC	OC	
42	High		Yes	cc-RCC	High	Fast and intense	Middle	cc-RCC	OC	
43	Middle	Ch-RCC	Yes		High	Mid and delayed	Yes	Ch-RCC	cc-RCC	
44	Low		Yes	AML	High	Slow	Middle	AML	p-RCC	

pRCC: Papillary renal cell carcinoma, ccRCC: Clear cell renal cell carcinoma, OC: Oncocytoma, ChRCC: Chromophobe renal cell carcinoma, AML: Angiomyolipoma, pRCC: Papillary renal cell carcinoma, ADC: Apparent diffusion coefficient, DCE: Dynamic contrast enhanced, T1w: T1-weighted, MRI: Magnetic resonance imaging

with an assessment of signal intensity compared to the renal cortex in the T2-weighted non-fat suppressed images, but unlike Cornelis *et al.*'s algorithm, the isointense or medium signal intensity does not narrow down the possibilities of

the subtypes to one specific type.<sup>[24]</sup> According to Cornelis *et al.*'s algorithm, an isointense or medium signal intensity using T2w denotes a subtype of Ch-RCC, and in our study, a total of 11 tumors were categorized as Ch-RCC after this

**Table 5:** Retrospective analysis of the MRI results divided by tumor subtypes (*n*=43\*).

T2	Hyperintense (%)	Isointense (%)	Hypointense (%)	Cornelis algorithm
Malignant ( <i>n</i> =29)	5 (17.2)	11 (37.9)	13 (44.9)	-
ccRCC ( <i>n</i> =24)	5 (20.8)	10 (41.7)	9 (37.5)	High
pRCC ( <i>n</i> =4)	-	-	4 (100.0)	Low
chRCC ( <i>n</i> =1)	-	1 (100.0)	-	Middle
Benign ( <i>n</i> =14)	9 (64.3)	1 (7.1)	4 (28.6)	-
OC ( <i>n</i> =12)	9 (75.0)	-	3 (25.0)	High
AML ( <i>n</i> =2)	-	1 (50.0)	1 (50.0)	Low
Dual Chemical shift	Yes	No	NR	
Malignant ( <i>n</i> =29)	26 (89.7)	2 (6.9)	1 (3.4)	-
ccRCC ( <i>n</i> =24)	22 (91.7)	1 (4.2)	1 (4.2)	Yes
pRCC ( <i>n</i> =4)	3 (75.0)	1 (25.0)	-	No
chRCC ( <i>n</i> =1)	1 (100.0)	-	-	N/A
Benign ( <i>n</i> =14)	13 (92.9)	-	1 (7.2)	-
OC ( <i>n</i> =12)	12 (100)	-	-	No
AML ( <i>n</i> =2)	1 (50.0)	-	1 (50.0)	Yes
DWI	High	Middle	Low	
Malignant ( <i>n</i> =29)	16 (55.2)	10 (34.5)	3 (10.3)	-
ccRCC ( <i>n</i> =24)	12 (50)	10 (41.7)	2 (8.3)	High
pRCC ( <i>n</i> =4)	3 (75.0)	-	1 (25.0)	Low
chRCC ( <i>n</i> =1)	1 (100.0)	-	-	Middle
Benign ( <i>n</i> =14)	10 (71.4)	4 (28.6)	-	-
OC ( <i>n</i> =12)	9 (75.0)	3 (25.0)	-	High
AML ( <i>n</i> =2)	1 (50.0)	1 (50.0)	-	Low
DCE-T1w wash-in	Fast and intense	Mid and delayed	Slow	
Malignant ( <i>n</i> =29)	12 (41.4)	8 (27.6)	9 (31.0)	-
ccRCC ( <i>n</i> =24)	12 (50.0)	7 (29.2)	5 (20.8)	Fast and intense
pRCC ( <i>n</i> =4)	-	1 (25.0)	3 (75.0)	Slow
chRCC ( <i>n</i> =1)	-	-	1 (100.0)	Mid and delayed
Benign ( <i>n</i> =14)	8 (57.1)	4 (28.6)	1 (7.1)	-
OC ( <i>n</i> =12)	7 (58.3)	4 (33.3)	1 (8.3)	Mid and delayed
AML ( <i>n</i> =2)	1 (50.0)	1 (50.0)	-	Fast and intense
DCE-T1w wash-out	Yes	Mid	No	
Malignant ( <i>n</i> =29)	4 (13.8)	13 (44.8)	12 (41.4)	-
ccRCC ( <i>n</i> =24)	4 (16.7)	12 (50.0)	8 (33.3)	Yes
pRCC ( <i>n</i> =4)	-	1 (25.0)	3 (75.0)	No
chRCC ( <i>n</i> =1)	-	-	1 (100.0)	Mid
Benign ( <i>n</i> =14)	4 (28.6)	9 (64.3)	1 (7.1)	-
OC ( <i>n</i> =12)	3 (25.0)	9 (75.0)	-	Mid
AML ( <i>n</i> =2)	1 (50.0)	-	1 (50)	Yes

AML: Angiomyolipoma, \* Including a total of 43 tumours. The mixed tumour was excluded in this part of the analysis, ccRCC: Clear cell renal cell carcinoma, ccRCC: Clear cell renal cell carcinoma, OC: Oncocytoma, ChRCC: Chromophobe renal cell carcinoma, pRCC: Papillary renal cell carcinoma, ADC: Apparent diffusion coefficient, DCE: Dynamic contrast enhanced, T1w: T1-weighted, MRI: Magnetic resonance imaging

first sequence assessment. Kay *et al.* only excluded AML in the isointense assessment of the T2w sequence, and ccRCC, which accounts for a majority of the malignant tumor subtypes, can have all three categoric appearances (high, isointense, and low), although most commonly showing high or isointense T2w patterns. This finding supports previous publications describing ccRCC's presentation using MRI but contradicts Cornelis' algorithm.<sup>[25,26]</sup>

A limitation of not only Kay *et al.*, but most of the studies proposing MRI as a diagnostic tool for differentiating tumor subtypes, is the retrospective design and the results being presented as sensitivity, specificity, positive predictive values, and negative predictive values.<sup>[24,27-30]</sup> Most of the studies initiate the conduct of their study with the histopathological results and then divide the MRI assessment and features based on the histopathological findings, instead of providing

prospective assessments. This design could affect and change the prevalence of the different subtypes which will affect the positive and negative predictive values. In addition, the sensitivities and specificities are calculated and presented for each tumor subtype, which is relevant for research purposes but is of limited interest in a clinical setting. Our prospective validation and cohort were not designed to explore sensitivities or specificities of incorrect diagnoses with MRI as a diagnostic test and histopathological examination as the gold standard.

Another issue that needs to be addressed when considering implementing image-guided characterization of tumor subtypes is interrater reliability. In our cohort, the assessments were done in agreement between two radiologists, and in the study, we did not explore inter- or intra-reader reliability. Several studies examine the interrater reliability or agreement (between observers), or intraobserver agreement (within observers) for ADC values or assessment of hypo-, iso-, or hypointense tumor profiles.<sup>[31-33]</sup> The literature suggests that such agreement varies from moderate to substantial, with the highest kappa values for ccRCC and pRCC.<sup>[24]</sup> When exploring a new diagnostic method with the potential to decrease the number of invasive procedures, the inter- and intraobserver agreement needs to be sufficient to avoid errors, and diagnostic accuracy must be explored not only for subspecialists with research and/or clinical interest in MRI subtyping but for the common radiologist working with MRI and renal tumors.

No clear guidelines or recommendations exist for the use of MRI in the diagnostic work-up, staging, or follow-up.<sup>[34-36]</sup> The ESMO guideline for clinical practice for diagnosis, treatment, and follow-up of RCC states “MRI may provide additional information in investigating local advancement and venous involvement by tumor thrombus.”<sup>[34]</sup> In clinical practice, MRI plays an important role in the treatment of patients where contrast-enhanced CT is contraindicated; however, exploiting the highest potential of MRI also requires intravenous contrast.

Despite the small sample size ( $n = 30$ ), the frequency of the RCC subtypes reported elsewhere (ccRCC: 80–90%, pRCC: 10–15%, and chRCC: 4–5%<sup>[37]</sup>) was similar to the findings in this study (ccRCC: 80.0%, pRCC: 13.3%, and chRCC: 3.3%). Literature reports a 1.5:1 predominance for men over women to be diagnosed with a renal tumor, with peak incidence occurring between 60 and 70 years of age.<sup>[37]</sup> This study had a male: female ratio of 2.4:1 and a mean age of 66 years. Despite this difference, this study’s prospective collected sample was considered a representative sample of the true population. Three patients were excluded from the study population due to inconclusive histopathology from biopsy. The European Association of Urology guidelines for RCC from 2019 presented a similar range

for non-diagnostic biopsies of 2.5–22%,<sup>[36]</sup> which again demonstrated that the study sample was representative of the true population.

We present the first prospective validation study exploring the Cornelis *et al.* algorithm for the use of multiparametric MRI to differentiate between renal tumors. Despite being unable to reproduce the results, the findings are relevant for future work and progress on using MRI for image classification of renal tumors. This study does have several limitations. Radiographers reported the time from contrast injection to manually initiating the time of T1w DIXON as between 25 s and 120 s. Ideally, this interval could have been standardized if manual monitoring had been avoided. Secondly, the small sample size of only 44 renal tumors could also limit the results of this study. However, the distribution of subtypes was consistent with the epidemiologically reported frequencies. Thirdly, according to the literature, there was a potential risk of misdiagnosing when relying solely on core biopsy, where only 86–98% are diagnostically accurate.<sup>[38,39]</sup> Excisional biopsy material was available in most cases ( $n = 29$ ) in this study, but in cases where the core biopsy diagnosed a benign renal tumor ( $n = 6$ ) or for the tumors receiving cryoablation ( $n = 15$ ), the diagnosis depended solely on the core biopsy and therefore there existed a potential risk of misdiagnosing. This was especially true concerning OC s, where biopsies are not always able to determine exact diagnosis, but only point in the direction of oncocyctic neoplasm. However, as all histopathology reports were re-evaluated by the same pathologist, the risk of misdiagnosing was considered limited, and histopathology could still be considered the gold standard.

## CONCLUSION

We aimed to prospectively validate a multiparametric MRI algorithm for classifying renal tumors but could not reproduce the results from the original study. The MRI algorithm shows few promising results to categorize renal tumors, and histopathological examinations are still needed for clinical decisions and follow-up regimes of renal masses.

### Declaration of patient consent

The authors certify that they have obtained all appropriate patient consent.

### Financial support and sponsorship

Nil.

### Conflicts of interest

There are no conflicts of interest.

## REFERENCES

- Du Z, Chen W, Xia Q, Shi O, Chen Q. Trends and projections of kidney cancer incidence at the global and national levels, 1990-2030: A Bayesian age-period-cohort modeling study. *Biomark Res* 2020;8:16.
- Znaor A, Lortet-Tieulent J, Laversanne M, Jemal A, Bray F. International variations and trends in renal cell carcinoma incidence and mortality. *Eur Urol* 2015;67:519-30.
- Motzer RJ, Bander NH, Nanus DM. Renal-cell carcinoma. *N Engl J Med* 1996;335:865-75.
- Hsieh JJ, Purdue MP, Signoretti S, Swanton C, Albiges L, Schmidinger M, *et al.* Renal cell carcinoma. *Nat Rev Dis Primers* 2017;3:17009.
- Flanigan RC, Campell SC, Clark JI, Picken MM. Metastatic renal cell carcinoma. *Curr Treat Options in Oncol* 2003;4:385-90.
- Cheville JC, Lohse CM, Zincke H, Weaver AL, Blute ML. Comparisons of outcome and prognostic features among histologic subtypes of renal cell carcinoma. *Am J Surg Pathol* 2003;27:612-24.
- Taouli B, Thakur RK, Mannelli L, Babb JS, Kim S, Hecht EM, *et al.* Renal lesions: Characterization with diffusion-weighted imaging versus contrast-enhanced MR imaging. *Radiology* 2009;251:398-407.
- Kim S, Jain M, Harris AB, Lee VS, Babb JS, Sigmund EE, *et al.* T1 Hyperintense renal lesions: Characterization with diffusion-weighted MR imaging versus contrast-enhanced MR imaging. *Radiology* 2009;251:796-807.
- Mytsyk Y, Dutka I, Borys Y, Komnatska I, Shatynska-Mytsyk I, Farooqi AA, *et al.* Renal cell carcinoma: Applicability of the apparent coefficient of the diffusion-weighted estimated by MRI for improving their differential diagnosis, histologic subtyping, and differentiation grade. *Int Urol Nephrol* 2017;49:215-24.
- Schneider A, Probst T, Kirchin MA, Stroeder J, Fries P, Buecker G. Low-dose gadobenate dimeglumine-enhanced MRI of the kidney for the differential diagnosis of localized renal lesions. *Radiol Med* 2015;120:1100-11.
- Sandrasegaran K, Sundaram CP, Ramaswamy R, Akisik FM, Rydberg MP, Lin C, *et al.* Usefulness of diffusion-weighted imaging in the evaluation of renal masses. *AJR Am J Roentgenol* 2010;194:438-45.
- Dodelzon K, Mussi TC, Babb JS, Taneja SS, Rosenkrantz AB. Prediction of growth rate of solid renal masses: Utility of mr imaging features-preliminary experience. *Radiology* 2012;262:884-93.
- Pedrosa I, Chou MT, Ngo L, Baroni RH, Genega EM, Galaburda L, *et al.* MR classification of renal masses with pathologic correlation. *Eur Radiol* 2008;18:365-75.
- Wang H, Cheng L, Zhang X, Wang D, Guo A, Gao Y, *et al.* Renal cell carcinoma: Diffusion-weighted MR imaging for subtype differentiation at 3.0 T. *Radiology* 2010;257:135-43.
- Sun MR, Ngo L, Genega EM, Atkins MB, Finn ME, Rofsky NM, *et al.* Renal cell carcinoma: Dynamic contrast-enhanced MR imaging for differentiation of tumor subtypes--correlation with pathologic findings. *Radiology* 2009;250:793-802.
- Cornelis F, Lasserre AS, Tournias T, Deminiere C, Ferriere JM, Le Bras Y, *et al.* Combined late gadolinium-enhanced and double-echo chemical-shift MRI help to differentiate renal oncocytomas with high central T2 signal intensity from renal cell carcinomas. *AJR Am J Roentgenol* 2013;200:830-8.
- Low G, Huang G, Fu W, Moloo Z, Girgis S. Review of renal cell carcinoma and its common subtypes in radiology. *World J Radiol* 2016;8:484-500.
- Cornelis F, Grenier N. Multiparametric magnetic resonance imaging of solid renal tumors: A practical algorithm. *Semin Ultrasound CT MR* 2017;38:47-58.
- von Elm E, Altman DG, Egger M, Pocock SJ, Gotsche PC, Vandenbroucke JP, *et al.* The Strengthening the Reporting of Observational Studies in Epidemiology (STROBE) statement: Guidelines for reporting observational studies. *Int J Surg* 2014;12:1495-9.
- Harris PA, Taylor R, Thielke R, Payne J, Gonzalez N, Conde JG. Research electronic data capture (REDCap)--a metadata-driven methodology and workflow process for providing translational research informatics support. *J Biomed Inform* 2009;42:377-81.
- Vendrami CL, Villavicencio CP, DeJulio TJ, Chatterjee A, Casalino DD, Horowitz JM, *et al.* Differentiation of solid renal tumors with multiparametric MR imaging. *Radiographics* 2017;37:2026-42.
- Canvasser NE, Kay FU, Xi Y, Pinho DE, Costa D, de Leon AD, *et al.* Diagnostic accuracy of multiparametric magnetic resonance imaging to identify clear cell renal cell carcinoma in cT1a renal masses. *J Urol* 2017;198:780-6.
- Rossi SH, Prezzi D, Kelly-Morland C, Goh V. Imaging for the diagnosis and response assessment of renal tumours. *World J Urol* 2018;36:1927-42.
- Kay FU, Canvasser NE, Xi Y, Pinho DE, Costa DN, de Leon AD, *et al.* Diagnostic performance and interreader agreement of a standardized MR imaging approach in the prediction of small renal mass histology. *Radiology* 2018;287:543-53.
- Prasad SR, Humphrey PA, Catena JR, Narra VR, Srigley JR, Cortez AD, *et al.* Common and uncommon histologic subtypes of renal cell carcinoma: Imaging spectrum with pathologic correlation. *Radiographics* 2006;26:1795-806; discussion 1806-10.
- Campbell N, Rosenkrantz AB, Pedrosa I. MRI phenotype in renal cancer: Is it clinically relevant? *Top Magn Reson Imaging* 2014;23:95-115.
- Hotker AM, Mazaheri Y, Wibmer A, Zheng J, Moskowicz CS, Tickoo SK, *et al.* Use of DWI in the differentiation of renal cortical tumors. *AJR Am J Roentgenol* 2016;206:100-5.
- Pitra T, Pivovarcikova K, Tupy R, Alaghehbandan R, Barakova T, Travnicek I, *et al.* Magnetic resonance imaging as an adjunct diagnostic tool in computed tomography defined Bosniak IIF-III renal cysts: A multicenter study. *World J Urol* 2018;36:905-11.
- Ferreira AM, Reis RB, Kajiwarra PP, Silva GE, Elias J Jr., Muglia VF. MRI evaluation of complex renal cysts using the Bosniak classification: A comparison to CT. *Abdom Radiol (NY)* 2016;41:2011-9.
- Jhaveri KS, Elmi A, Hosseini-Nik H, Hedgire S, Evans A, Jewett M, *et al.* Predictive value of chemical-shift MRI in distinguishing clear cell renal cell carcinoma from non-clear

- cell renal cell carcinoma and minimal-fat angiomyolipoma. *AJR Am J Roentgenol* 2015;205:W79-86.
31. Ludwig DR, Ballard DH, Shetty AS, Siegel CL, Yano M. Apparent diffusion coefficient distinguishes malignancy in T1-hyperintense small renal masses. *AJR Am J Roentgenol* 2020;214:114-21.
  32. Ponhold L, Javor D, Heinz-Peer G, Sevcenco S, Hofstetter M, Baltzer PA. Inter-observer variation and diagnostic efficacy of apparent diffusion coefficient (ADC) measurements obtained by diffusion-weighted imaging (DWI) in small renal masses. *Acta Radiol* 2016;57:1014-20.
  33. Schieda N, Lim RS, McInnes MD, Thomassin I, Renard-Penna R, Tavoraro S, *et al.* Characterization of small (<4cm) solid renal masses by computed tomography and magnetic resonance imaging: Current evidence and further development. *Diagn Interv Imaging* 2018;99:443-55.
  34. Escudier B, Porta C, Schmidinger M, Rioux-Leclercq N, Bex A, Khoo V, *et al.* Renal cell carcinoma: ESMO Clinical Practice Guidelines for diagnosis, treatment and follow-up. *Ann Oncol* 2019;30:706-20.
  35. Campbell S, Uzzo RG, Allaf ME, Bass EB, Cadeddu JA, Chang A, *et al.* Renal mass and localized renal cancer: AUA guideline. *J Urol* 2017;198:520-9.
  36. Ljungberg B, Albiges L, Abu-Ghanem Y, Bensalah K, Dabestani S, Fernandez-Pello S, *et al.* European association of urology guidelines on renal cell carcinoma: The 2019 update. *Eur Urol* 2019;75:799-810.
  37. Ljungberg B, Bensalah K, Canfield S, Dabestani S, Hofmann F, Hora M, *et al.* EAU guidelines on renal cell carcinoma: 2014 update. *Eur Urol* 2015;67:913-24.
  38. Neuzillet Y, Lechevallier E, Andre M, Daniel L, Coulange C. Accuracy and clinical role of fine needle percutaneous biopsy with computerized tomography guidance of small (less than 4.0 cm) renal masses. *J Urol* 2004;171:1802-5.
  39. Volpe A, Finelli A, Gill IS, Jewett MA, Martignoni G, Polascik TJ, *et al.* Rationale for percutaneous biopsy and histologic characterisation of renal tumours. *Eur Urol* 2012;62:491-504.

**How to cite this article:** Pietersen PI, Lynggård Bo Madsen J, Asmussen J, Lund L, Nielsen TK, Pedersen M, *et al.* Multiparametric magnetic resonance imaging for characterizing renal tumors: A validation study of the algorithm presented by Cornelis *et al.* *J Clin Imaging Sci* 2023;13:7.